Development 137, 755-765 (2010) doi:10.1242/dev.045757

SIX1 acts synergistically with TBX18 in mediating ureteral smooth muscle formation

Xuguang Nie[1], Jianbo Sun[1], Ronald E. Gordon[2], Chen-Leng Cai[3,4,5] and Pin-Xian Xu[1,3,*]

SUMMARY

Dysfunction of the ureter often leads to urine flow impairment from the kidney to the bladder, causing dilation of the ureter and/or renal pelvis. *Six1* is a crucial regulator of renal development: mutations in human *SIX1* cause branchio-oto-renal (BOR) syndrome and *Six1*$^{-/-}$ mice exhibit renal agenesis, although the ureter is present. It remains unclear whether *Six1* plays a role in regulating ureter morphogenesis. We demonstrate here that *Six1* is differentially expressed during ureter morphogenesis. It was expressed in undifferentiated smooth muscle (SM) progenitors, but was downregulated in differentiating SM cells (SMCs) and had disappeared by E18.5. In *Six1*$^{-/-}$ mice, the ureteral mesenchymal precursors failed to condense and differentiate into normal SMCs and showed increased cell death, indicating that *Six1* is required for the maintenance and normal differentiation of SM progenitors. A delay in SMC differentiation was observed in *Six1*$^{-/-}$ ureters. A lack of *Six1* in the ureter led to hydroureter and hydronephrosis without anatomical obstruction when kidney formation was rescued in *Six1*$^{-/-}$ embryos by specifically expressing *Six1* in the metanephric mesenchyme, but not the ureter, under control of the *Eya1* promoter. We show that *Six1* and *Tbx18* genetically interact to synergistically regulate SMC development and ureter function and that their gene products form a complex in cultured cells and in the developing ureter. Two missense mutations in *SIX1* from BOR patients reduced or abolished SIX1-TBX18 complex formation. These findings uncover an essential role for *Six1* in establishing a functionally normal ureter and provide new insights into the molecular basis of urinary tract malformations in BOR patients.

KEY WORDS: *Six1*, *Tbx18*, Ureter, Smooth muscle, Proliferation, Apoptosis, Hydroureter, Mouse

INTRODUCTION

Developmental disorders of the ureter constitute a significant portion of CAKUT (congenital anomalies of the kidney and urinary tract anomalies), a major cause of chronic renal failure in children (Hosgor et al., 2005; Kuwayama et al., 2002; Schedl, 2007; Shah et al., 2004). For example, functional impairment of the ureteric smooth muscle (SM) is a common cause of renal dysfunction, leading to a failure of urine transport from the renal pelvis to the bladder, often resulting in dilation of the ureter (hydroureter) and renal pelvis (hydronephrosis), which may ultimately lead to renal failure.

In mammals, ureter and kidney development begins when an epithelial outgrowth (the ureteric bud, UB) appears from the caudal end of the Wolffian duct through inductive interactions with adjacent metanephric mesenchyme (MM) (Dressler, 2006; Saxen et al., 1986). In mice, this process occurs at ~E10.5 and soon after its formation, the nascent UB continues to grow towards the MM and divides into tip and trunk regions in response to local signals from the surrounding mesenchyme (Brenner-Anantharam et al., 2007). Subsequently, the proximal tip region of the UB further invades the MM and undergoes repeated branching morphogenesis to form the intra-renal collecting system (Costantini, 2006; Shah et al., 2004), while the trunk of the UB elongates to form the ureteric epithelium, which is the urothelium that lies outside the kidney.

During elongation, the urothelium recruits cells from the intermediate mesenchyme and tailbud mesenchyme to surround the epithelial tube (Brenner-Anantharam et al., 2007). The ureteral mesenchymal cells are constantly expanded to provide a cellular resource for continuous ureter elongation. Interaction of these mesenchyme cells with urothelium is required for proper morphogenesis of the ureter. In response to signals from the epithelium, the mesenchyme becomes organized into different cell layers (Yu et al., 2002). The subpopulation of mesenchymal cells located immediately adjacent to the urothelium forms a loose stromal cell layer, and these cells express high levels of patched (*Ptch*), which serves as a readout for response to SHH signaling from the epithelium. This layer also expresses BMP4, which promotes elongation of the urothelium and differentiation of the surrounding mesenchyme. Cells in this layer later give rise to laminar propria as well as to stromal cells within the developing ureter. The mesenchymal cells located outside of this stromal cell layer condense to form ureteral SM. Mesenchymal condensation for SM is evident at embryonic day (E) 13.5 and SM cell (SMC) differentiation initiates from ~E15.0 in a proximal-distal wave (Yu et al., 2002). The outermost layer of the mesenchyme matures into a connective tissue coating that contains fibrocytes.

The molecular mechanisms controlling ureter development are only beginning to be elucidated. Epithelial SHH and WNT signaling and mesenchymal BMP4 signaling are known to regulate epithelial-mesenchymal interactions during ureter development (Brenner-Anantharam et al., 2007; Cain et al., 2008; Carroll et al., 2005; Michos et al., 2007; Miyazaki et al., 2000; Raatikainen-Ahokas et al., 2000; Wang et al., 2009; Yu et al., 2002). Recently, two transcription factors, the T-box protein TBX18 and the zinc-finger protein teashirt 3 (TSHZ3), have been shown to be expressed in SMC precursors and to be important for SMC differentiation (Airik et al., 2006; Caubit et al., 2008). How

[1]Departments of Genetics and Genomic Sciences, [2]Pathology and [3]Developmental and Regenerative Biology, [4]Center for Molecular Cardiology, [5]Black Family Stem Cell Institute, Mount Sinai School of Medicine of New York University, New York, NY 10029, USA.

*Author for correspondence (pinxian.xu@mssm.edu)

Accepted 23 December 2009

these signaling pathways and transcription factors act together to coordinate SMC specification and differentiation is poorly understood. Since these factors and different pathways are unlikely to be linear cascades, it will be necessary to determine how different pathways are organized into complex signaling networks that ultimately generate precise responses within ureteral mesenchymal precursor cells.

The murine homeobox Six gene family, which is homologous to the *Drosophila sine oculis*, plays essential roles in urinary tract development. Haploinsufficiency for human *SIX1* or *SIX5* leads to branchio-oto-renal (BOR) syndrome (Hoskins et al., 2007; Ruf et al., 2004), and ~6% of BOR patients show severe renal defects, including hydronephrosis and hydroureter/megaureter (Izzedine et al., 2004). We and others have previously shown that a lack of *Six1* in mice leads to renal agenesis, but that the ureter is still formed in $Six1^{-/-}$ mice (Li et al., 2003; Xu et al., 2003). A recent in vitro analysis indicated that the $Six1^{-/-}$ ureter is capable of expressing α-smooth muscle actin (SMA) when cultured in medium (Bush et al., 2006). However, it remains unclear whether SMA production is normal in the $Six1^{-/-}$ mutant. In addition, the etiology of the hydronephrosis and hydroureter/megaureter that occur in BOR syndrome is currently unclear.

In this study, we address whether *Six1* plays a role during ureter morphogenesis. We found that during ureter development, *Six1* is expressed in undifferentiated mesenchymal progenitors but its expression is downregulated in differentiating mesenchymal cells. In $Six1^{-/-}$ ureters, the mesenchymal cells failed to aggregate and differentiate normally and showed increased cell death. Furthermore, we demonstrate that loss of *Six1* function specifically in the ureter leads to hydroureter and hydronephrosis when the kidney is rescued in $Six1^{-/-}$ embryos. Finally, we show that *Six1* genetically interacts with *Tbx18* during ureter morphogenesis and that their gene products physically interact to form a complex both in vitro and in vivo. Our results uncovered an essential role for *Six1* during ureter patterning and provide new insights into the molecular basis for the urinary tract abnormalities that occur in BOR patients.

MATERIALS AND METHODS

Mice and genotyping

The $Six1^{+/-}$ ($Six1^{lacZ/+}$) mutation in a 129 strain (Laclef et al., 2003; Xu et al., 2003) and the $Tbx18^{GFP}$ mutation in a CD1 strain (Cai et al., 2008) were used. Genotyping was as described (Cai et al., 2008; Laclef et al., 2003; Xu et al., 2002). *Hoxb7-GFP* transgenic mice were also used (Srinivas et al., 1999).

Histology, X-gal staining, in situ hybridization, immunohistochemistry, transmission electron microscopy and explant culture

Histological examination, X-gal staining, whole-mount and section in situ hybridization were carried out according to standard procedures, with digoxigenin-labeled riboprobes specific for *Bmp4*, *Tbx18*, *Ptch1*, *Shh*, *Raldh2* and *SM22α*. We used six embryos of each genotype at each stage for each probe.

Antibodies for immunohistochemistry were as follows: mouse monoclonal anti-uroplakin IIIa (kindly provided by Dr T.-T. Sun, New York University, New York, USA), polyclonal anti-αSMA (NatuTec), monoclonal alkaline phosphatase (AP)-conjugated anti-αSMA (Sigma), polyclonal anti-SMMHC (Sigma) and anti-pSMAD1/5/8 (Cell Signaling). Fluorescent or HRP-conjugated secondary antibody was used for detection; the primary anti-αSMA antibody was detected using BCIP/NBT or DAB.

Transmission electron microscopy (TEM) was performed according to standard procedures.

Urinary tracts were isolated from E14.5 mouse embryos and cultured in Transwell dishes for 3-5 days for the peristaltic analysis.

TUNEL and BrdU-labeling assays

The TUNEL assay was performed as described (Xu et al., 1999). The BrdU-labeling experiment was performed as described (Zheng et al., 2003). HRP-conjugated secondary antibody was used for detection.

Transfection, co-immunoprecipitation (co-IP) and western blot

Transfection of HEK 293 cells, preparation of cell lysates, co-IP and western blot were performed as described (Buller et al., 2001).

For in vivo interaction, cell extracts from E13.5-14.5 ureters were prepared according to standard procedures. Approximately 3 mg of total protein was incubated with mouse anti-SIX1 or goat anti-TBX18 antibody and precipitated with protein A- or G-agarose beads for co-IP.

RESULTS

Six1 is expressed in ureteral mesenchyme

To examine whether *Six1* plays a direct role during ureter development, we first analyzed its spatiotemporal expression in the developing ureter from E10.5-P0. Since the mutant mice contain a *lacZ* gene driven by the *Six1* promoter, and the inserted *lacZ* transgene displayed a pattern identical to the *Six1* mRNA distribution obtained by in situ hybridization (Chen et al., 2009; Laclef et al., 2003; Xu et al., 2003; Zheng et al., 2003), we stained for β-galactosidase activity in $Six1^{lacZ}$ heterozygotes. *Six1* expression was observed in the ureteral mesenchyme from ~E12.5 (Fig. 1A) and was upregulated between E13.5 and E15.5 (Fig. 1B-D). In the ureteral mesenchyme, *Six1*-expressing cells were distributed in the inner layer that will differentiate into SM and in the outer layer that will mature into connective tissue (Fig. 1C,D). However, its expression was downregulated after E15.5, when the progenitors begin their differentiation (Fig. 1E,F), and became undetectable at ~E18.5 (data not shown) and P0 (Fig. 1G,H). Consistent with our previous observations (Xu et al., 2003), we detected some *lacZ*-positive cells in the collecting tubules of the kidney at E17.5 (Fig. 1E, arrow), but this expression was transient and had disappeared by E18.5-P0 (data not shown). By contrast, *lacZ*-positive cells were detected in the urothelium and the proximal tubules of the kidney at E18.5-P0 (Fig. 1G,H and data not shown). Our observation of *Six1* expression in the ureteral mesenchyme suggests that it might have a direct role in regulating ureter SMC development.

$Six1^{-/-}$ mice show malformation of ureteral SM

Inspection of freshly prepared specimens at P0 showed that, in most cases, $Six1^{-/-}$ ureters were truncated but their width appeared to be increased when compared with littermate controls [Fig. 2; diameter of the *Six1*-heterozygous ureter, 155±15.5 μm (n=6); diameter of the *Six1*-homozygous ureter, 179±30.9 μm (n=6); P=0.85]. Histological analysis revealed that the SM layer of control ureters had developed into a well-organized SM ring surrounding the urothelium, while the outer mesenchymal layer had matured into a connective coating containing sparsely distributed fibrocytes (Fig. 2C,E). By contrast, in $Six1^{-/-}$ ureters, the SM ring-like structure was formed but the SMCs were less differentiated and were more loosely condensed (Fig. 2D,F), while the outer layer of the mesenchymal cells also appeared to be more loosely distributed than in controls, which was more obvious in the proximal portion (Fig. 2D, arrow). In addition, the multilayered urothelium was noticeably disorganized in the mutant (Fig. 2C-F).

To determine the onset of ureter malformations in the mutant, we analyzed a developmental series of control and *Six1* mutant ureters. In $Six1^{+/-}$ controls, condensation of SMC progenitors was observed from as early as E12.5 (Fig. 2G,I,K). In the $Six1^{-/-}$ ureter, the mesenchymal condensation appeared to be delayed from E12.5 (Fig. 2H) and this layer appeared thicker on a radial

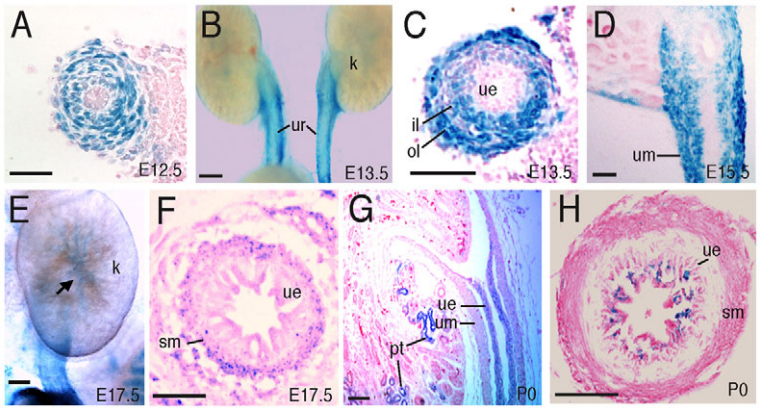

Fig. 1. Expression of *Six1* in the developing mouse ureter. Sections are X-gal stained for *lacZ* expression (blue). (**A**) A transverse section of E12.5 *Six1*$^{+/lacZ}$ ureter. (**B**) Whole-mount *Six1*$^{+/lacZ}$ kidney (k) and ureter (ur). (**C**) A transverse section of the ureter shown in B. (**D**) A longitudinal section of E15.5 *Six1*$^{+/lacZ}$ ureter. (**E**) Whole-mount E17.5 *Six1*$^{+/lacZ}$ kidney and ureter. (**F**) A transverse section of the ureter shown in E. (**G**) A longitudinal section of P0 *Six1*$^{+/lacZ}$ kidney and ureter. (**H**) A transverse section of the P0 *Six1*$^{+/lacZ}$ ureter. il, inner mesenchymal layer; ol, outer mesenchymal layer; pt, proximal tubules; sm, smooth muscle layer; ue, urothelium; um, ureteral mesenchyme. Scale bars: 50 μm.

plane than in the controls between E14.5 and 16.5 (Fig. 2J,L). The outer loose mesenchymal layer was also found to be thicker in the mutant than in controls. In addition, disorganization of the ureteric epithelial cells was noticeable from E16.5 (Fig. 2L, compare with 2K), at which stage *Six1* expression is not yet turned on in the epithelium. Since ureter morphogenesis requires mesenchymal-epithelial interactions, the epithelial defect observed at this early stage is most likely caused by defects in these interactions. These results indicate that normal patterning of the ureter requires *Six1* function.

SMCs fail to differentiate normally in the *Six1*$^{-/-}$ ureter

To determine the basis for the observed phenotypes, we performed marker gene and morphological analyses. Ureteral mesenchymal progenitors differentiate into SMCs in a proximal-to-distal wave starting at ~E15.0. We first examined whether SM differentiation is delayed in the mutant by analyzing the expression of SMA from E15.5. SMA was present along the entire length of the control ureters at this stage (Fig. 3A). By contrast, SMA was detected in the proximal region but was very faint in the distal ureters of *Six1*$^{-/-}$ littermate embryos (Fig. 3B). By E16.5, SMA was present along the entire length of the mutant ureters (data not shown), which is consistent with previous observations from cultured ureters (Bush et al., 2006). However, we observed an abnormal staining pattern for SMA in the mutant from E16.5 (Fig. 3C,D), which was not reported previously.

SMA-positive cells were spindle-shaped and appropriately aggregated to form the SM ring on transverse sections of control ureters at E16.5 (Fig. 3C), whereas SMA-positive cells were loosely aggregated, disorganized and not spindle-shaped in the mutant (Fig. 3D). *SM22*α (*Tagln* – Mouse Genome Informatics), which encodes a 22 kDa SMC lineage-restricted cytoskeletal protein, was strongly expressed in the differentiating SMCs at E16.5 (Fig. 3E). In *Six1*$^{-/-}$ ureters, *SM22*α expression was present but the number of *SM22*α-expressing cells was greatly reduced (Fig. 3F). At E18.5, SMA was detectable in *Six1*$^{-/-}$ ureters but SMA-positive cells were reduced in number and loosely associated (Fig. 3H, compare with 3G). Similarly, SM myosin heavy chain (SMMHC; MYH11 – Mouse Genome Informatics) expression was also observed in *Six1*$^{-/-}$ ureters at P0 but the SMMHC-positive cells were greatly reduced in number and disorganized (Fig. 3J) compared with controls (Fig. 3I). TEM further confirmed that SMCs were fewer, disorganized and irregularly shaped in *Six1*$^{-/-}$ ureter transverse sections (Fig. 3L, compare with 3K). In addition, TEM confirmed that there was a thicker outer layer of connective coating in the mutant (Fig. 3K,L). Together, these results demonstrate that *Six1* is required for normal SMC differentiation.

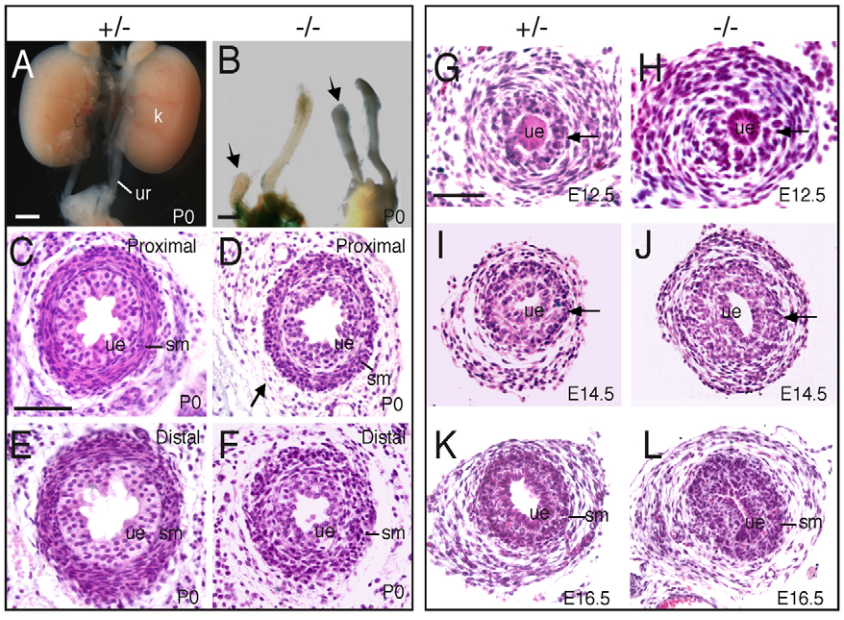

Fig. 2. Ureter anomalies in *Six1*$^{-/-}$ embryos. (**A**,**B**) Urinary tract systems in *Six1*$^{+/-}$ control (A) and *Six1*$^{-/-}$ (B) mouse embryos. Arrows point to truncation of the ureters (ur). B shows X-gal-stained (left) and unstained (right) urinary tract systems. (**C-F**) Transverse sections showing the proximal and distal regions of the *Six1*$^{+/-}$ (C,E) and *Six1*$^{-/-}$ (D,F) ureter. (**G-L**) Transverse sections of ureters in *Six1*$^{+/-}$ (G,I,K) and littermate *Six1*$^{-/-}$ (H,J,L) embryos from E12.5-16.5. Arrows point to condensing mesenchyme that forms the smooth muscle (sm) layer. ue, ureteric epithelium. Scale bars: 50 μm.

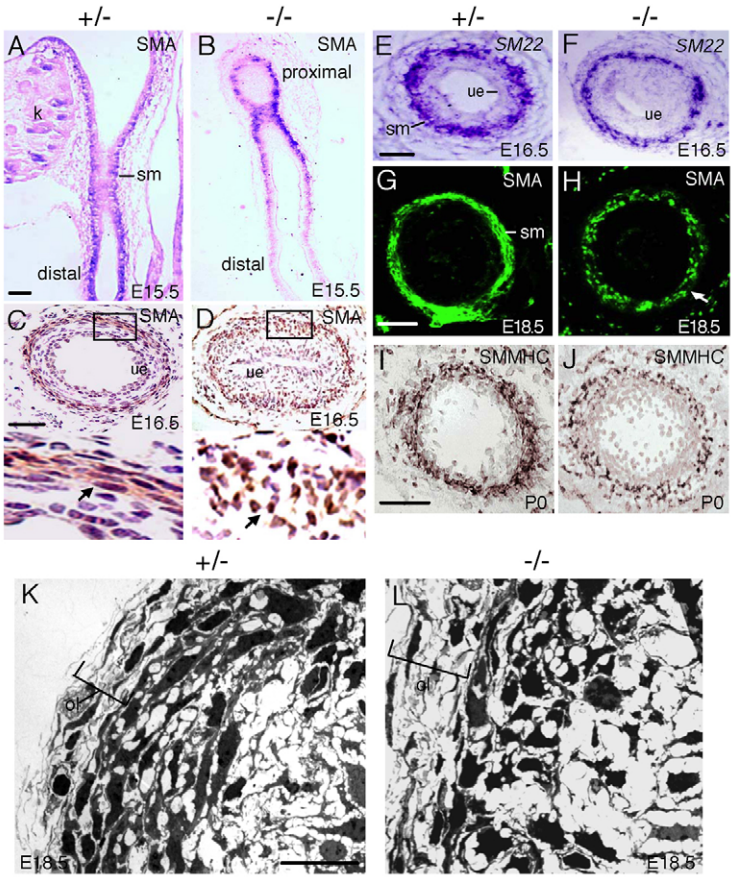

Fig. 3. Ureteric SMC differentiation in *Six1*$^{+/-}$ control and *Six1*$^{-/-}$ mouse ureters. (**A**,**B**) Longitudinal sections of the ureter showing SMA in the differentiating SMCs (detected using BCIP/NBT). (**C**,**D**) Transverse sections showing SMA staining (detected using DAB). The lower panels of C and D show higher magnification images of the boxed areas. Arrows point to spindle-shaped SMCs in control ureters and disoriented SMCs in *Six1*$^{-/-}$ ureters. (**E**,**F**) Transverse sections of proximal ureters showing *SM22*α expression in differentiating SMCs. (**G**,**H**) Transverse sections showing SMA staining. Arrow points to disoriented SMCs. (**I**,**J**) Transverse sections showing SMMHC staining. (**K**,**L**) Transmission electron micrographs of E18.5 ureter transverse sections. ol, outer layer of the ureteral mesenchyme. Scale bars: 50 μm in A-J; 10 μm in K,L.

We next examined a set of molecules that are essential for ureter SM development. *Tbx18*, a crucial regulator of the development of SMC precursors, is expressed in the periureteral mesenchymal cells from E11.5, and its expression is downregulated in differentiating SMCs (Airik et al., 2006). At ~E16.0, we found that *Tbx18*-expressing cells were distributed in the SM layer of the control ureter (Fig. 4A). However, more *Tbx18*-positive cells were observed in the SM layer of the *Six1*$^{-/-}$ ureter (Fig. 4B), suggesting that differentiation of the mesenchymal precursors into SMCs is delayed or that a subpopulation of SMC progenitors fails to undergo normal differentiation.

SHH signaling is necessary for normal SMC differentiation by regulating *Bmp4* expression in the mesenchyme (Yu et al., 2002). We found that *Shh* expression in the urothelium, as well as that of its downstream target gene *Ptch1* in the mesenchyme, appeared normal in *Six1*$^{-/-}$ ureters at E14.5-15.5 (Fig. 4C-F). *Bmp4* is expressed in the mesenchymal progenitors adjacent to the epithelium before SMC differentiation (Fig. 4G), and BMP4 signaling promotes SM formation in the ureter and kidney (Brenner-Anantharam et al., 2007; Wang et al., 2009). In the *Six1*$^{-/-}$ ureter, *Bmp4* expression appeared comparable to that of controls at E14.5 (Fig. 4H). We further examined the activity of BMP4 signaling by analyzing the expression of phosphorylated SMAD1/5/8 (pSMAD), which are established mediators of BMP signaling (Massague et al., 2005). No difference in pSMAD antigen staining was observed between control and *Six1*$^{-/-}$ ureters (data not shown). Similarly, the expression of the stromal cell marker retinaldehyde dehydrogenase (*Raldh2*; *Aldh1a2* – Mouse Genome Informatics) in the mesenchymal cell population between the urothelium and the SM layer was not detectably altered in the mutant at E18.5 (Fig. 4I,J). Thus, *Six1* does not appear to be required for the expression of *Shh*, *Ptch1*, *Bmp4* and *Raldh2* during ureter development.

Increased apoptosis in the developing *Six1*$^{-/-}$ ureter

Since the mutant ureters often had a thicker mesenchymal layer, especially in the proximal region (Fig. 2), we tested whether cell proliferation is altered by performing BrdU-incorporation experiments. We counted six serial sections of proximal and distal regions of each ureter separately and quantified the number of BrdU-positive cells. Compared with the control, more BrdU-positive cells were observed on transverse sections of the mutant ureter in both proximal and distal regions at E14.5-15.5 (Fig. 5A-D and data not shown). However, as the total number of ureteral mesenchymal cells is increased on a radial plane in the mutant, the proliferation rate in the condensing mesenchymal layer was comparable between control and mutant littermates (0.315±0.03 versus 0.323±0.04), whereas the outer layer of the mutant ureter showed a slightly higher rate of proliferation compared with the *Six1*-heterozygous littermate control (0.263±0.03 versus 0.22±0.01), while the proliferation rate was unaltered in the epithelium in the mutant ureter (Fig. 5E). Since the cell proliferation rate is comparable between control and mutant ureter, and as we often observed truncation of ureters in the mutant, the defect in mesenchymal expansion on a radial plane could be secondary to the elongation defect.

As we have previously found that loss of *Six1* leads to abnormal cell death in the otic vesicle, the olfactory epithelium and in the pharyngeal endoderm-derived organs (Zheng et al., 2003; Zou et al., 2006; Chen et al., 2009), it is possible that a subpopulation of the

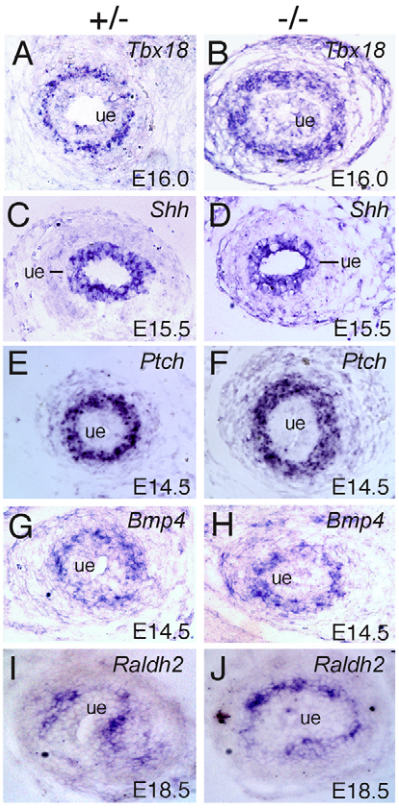

Fig. 4. Molecular marker analysis of *Six1*$^{-/-}$ ureteral mesenchyme. In situ hybridization on transverse sections of *Six1*$^{+/-}$ control and *Six1*$^{-/-}$ mouse ureters with (**A**,**B**) *Tbx18*, (**C**,**D**) *Shh*, (**E**,**F**) *Ptch1*, (**G**,**H**) *Bmp4* and (**I**,**J**) *Raldh2*. ue, ureteric epithelium.

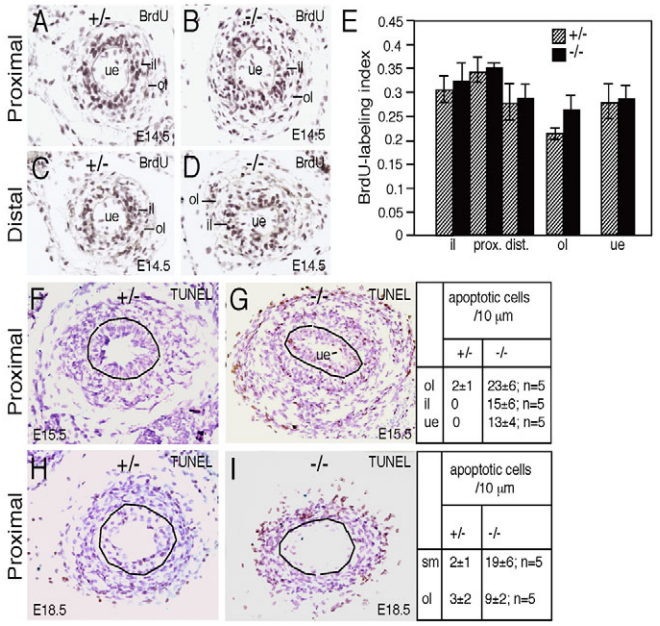

Fig. 5. Cell proliferation and apoptosis in *Six1*$^{-/-}$ ureters. (**A-D**) Cell proliferation analysis by BrdU staining on E14.5 *Six1*$^{+/-}$ control and *Six1*$^{-/-}$ mouse ureter transverse sections. (**E**) Statistical analysis of BrdU-positive cells. BrdU-positive cells and the total number of cells in each layer on each transverse section were counted and data from six sections from each ureter (from four ureters) were normalized as the BrdU labeling index. In the mesenchyme: P=0.1361, control inner layer (il) (0.31±0.03) versus mutant inner layer (0.323±0.04); P=0.0325, control proximal inner layer (prox.) (0.34±0.03) versus mutant proximal inner layer (0.35±0.01); P=0.0782, control distal inner layer (dist.) (0.28±0.04) versus mutant distal inner layer (0.29±0.03); P=0.0964, control outer layer (ol) (0.23±0.01) versus mutant outer layer (0.27±0.02). In E14.5 ureteric epithelium (ue): P=0.1927, control (0.28±0.04) versus mutant (0.29±0.03). P-values were calculated using StatView t-test; error bars indicate s.d. (**F-I**) TUNEL analysis of E15.5 and E18.5 *Six1*$^{+/-}$ control and *Six1*$^{-/-}$ ureters. TUNEL-positive cells (brown nuclei) were counted from five serial sections from each ureter (from at least six ureters). Shown are the average number of TUNEL-positive cells per (10 μm) section for each genotype. sm, smooth muscle layer.

ureteral mesenchymal cells degenerates and thus fails to form a normal SM layer. We therefore investigated whether the mesenchymal cells in the developing *Six1*$^{-/-}$ ureter undergo abnormal cell death. Transverse sections of E14.5-18.5 normal and mutant ureters (n=6) were processed for the TUNEL method of detecting apoptotic nuclei. No abnormal cell death was observed at E14.5 (data not shown). However, abnormal cell death in the ureteral mesenchyme of *Six1*$^{-/-}$ embryos was observed in the proximal region of the ureter from E15.5 (Fig. 5G). In addition, increased cell death was also observed in the urothelium (Fig. 5G). At E18.5, apoptotic cells were seen along the entire length of the ureter in *Six1*$^{-/-}$ embryos (Fig. 5I). By contrast, very few apoptotic cells were detected in the controls at these stages (Fig. 5F,H). Thus, *Six1* appears to regulate ureteral mesenchymal cell survival and the defective formation of SM in *Six1*$^{-/-}$ ureters can be attributed, at least in part, to increased cell death. The early onset of abnormal cell death observed in *Six1*$^{-/-}$ urothelium further indicates that the early mesenchymal *Six1* expression is also required for normal development of the urothelium.

Maturation of the urothelium is disturbed in the *Six1*$^{-/-}$ ureter

We further characterized the defect that might occur during differentiation of the mutant urothelium by immunostaining for uroplakin (UPK), a marker for differentiated urothelium (Sun et al., 1999). UPK expression was detected at the apical surface of the urothelium of control ureters at E16.5-18.5 (Fig. 6A,B). In *Six1*$^{-/-}$ ureters, despite the obvious disorganization of the urothelium, UPK expression was detectable at the apical surface at these stages (Fig. 6C,D). However, its expression was reduced in many areas of the mutant urothelium at E18.5 (Fig. 6D). The alteration in UPK expression could be a secondary effect of increased cell death as detected by the TUNEL assay. Nonetheless, our results suggest that *Six1* is not required for the initiation of UPK expression but might be necessary for its maintenance.

Six1$^{-/-}$ mice develop hydroureter and hydronephrosis when kidney development is rescued by *Six1* expression in MM

Although ~22-30% of *Six1*$^{-/-}$ mice had unilateral hypoplastic kidneys (n=50), no hydroureter was observed. Histological analysis revealed that the hypoplastic kidneys were extremely rudimentary, with only some tubule-like structures (data not shown), indicating that they were not functional. To determine whether the observed abnormal SM formation would lead to malfunction of the ureter in the presence of a functional kidney, we sought to rescue kidney development in *Six1*$^{-/-}$ embryos by generating *Eya1*^{Six1} knock-in

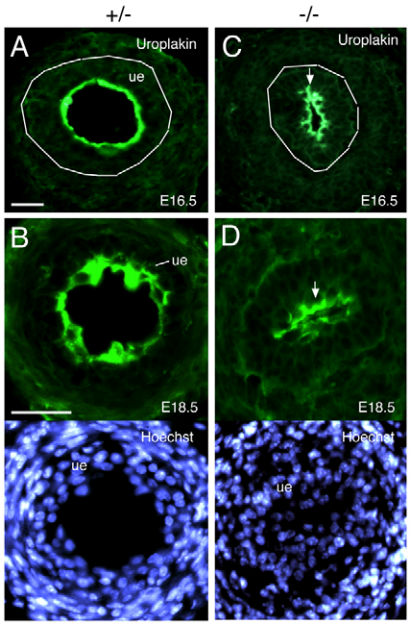

Fig. 6. Uroplakin expression in control and mutant ureters. Immunostaining for uroplakin IIIa (green) in urothelium (ue) of (**A**,**B**) *Six1*$^{+/-}$ and (**C**,**D**) *Six1*$^{-/-}$mouse embryos. Lower panels of B and D are counter-stained with Hoechst. Scale bars: 50 μm.

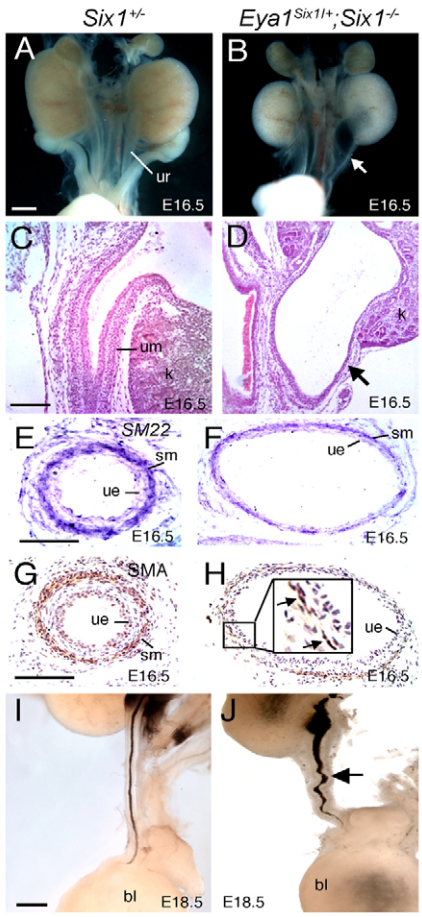

Fig. 7. Lack of *Six1* in the ureter leads to hydroureter and hydronephrosis. (**A**,**B**) Whole E16.5 urinary tracts from *Six1*$^{+/-}$ and *Eya1*$^{Six1/+}$;*Six1*$^{-/-}$ mouse embryos. Arrow points to hydroureter in *Eya1*$^{Six1/+}$;*Six1*$^{-/-}$. (**C**,**D**) Hematoxylin and Eosin-stained longitudinal sections of the kidney (k) and ureters shown in A and B. Arrow indicates the thin wall of ureteral mesenchyme (um) in the mutant. (**E-H**) In situ hybridization for *SM22α* (E,F) and immunostaining for SMA (G,H) on ureter transverse sections. Arrows in the higher magnification image in H point to SMCs. (**I**,**J**) E18.5 urinary tracts in which India ink was injected into the renal pelvis. Arrow points to dilated ureter in the *Eya1*$^{Six1/+}$;*Six1*$^{-/-}$ ureter. bl, bladder; ue, urothelium. Scale bars: 50 μm.

mice (see Fig. S1A,B in the supplementary material). Unlike *Six1*, *Eya1* is exclusively expressed in the MM and its expression is preserved in *Six1*$^{-/-}$ embryos at E9.5-10.5 (see Fig. S1C in the supplementary material) (Sajithlal et al., 2005; Xu et al., 2003). Thus, expression of *Six1* in the MM under the control of the *Eya1* promoter may rescue kidney development without affecting the ureter of *Six1*$^{-/-}$ embryos.

As expected, kidneys were always formed in *Eya1*$^{Six1/+}$;*Six1*$^{-/-}$ embryos (9/9), although they were often smaller than normal. Interestingly, hydronephrosis and hydroureter, either unilaterally or bilaterally, were often observed in the *Eya1*$^{Six1/+}$;*Six1*$^{-/-}$ embryos (~56%, 5/9) from as early as E16.5 (Fig. 7A,B). By contrast, the *Eya1*$^{lacZ/+}$;*Six1*$^{-/-}$ control mice (see Fig. S1A in the supplementary material) had no kidneys (data not shown), similar to what was observed in *Six1*$^{-/-}$ mice. Histological analysis confirmed dilation of the renal pelvis in the mutant (Fig. 7C,D). Staining with an *SM22α* in situ probe and anti-SMA antibody on the hydroureter transverse sections confirmed the presence of differentiating SMCs (Fig. 7E-H), although the structural organization of the muscular layer was disrupted. In contrast to the irregularly shaped SMA-positive cells in *Six1*$^{-/-}$ ureters (Fig. 3D), SMA staining revealed some spindle-shaped SMCs in *Eya1*$^{Six1/+}$;*Six1*$^{-/-}$ ureters (Fig. 7H), which could have resulted from the physical force associated with dilation. Similar to what was observed in *Six1*$^{-/-}$ ureters, early signaling for the development of SMC precursors was not affected in *Eya1*$^{Six1/+}$;*Six1*$^{-/-}$ ureters as judged by the expression of *Bmp4* and *Ptch1* before the onset of hydroureter and hydronephrosis (data not shown).

Analysis of E18.5 mutant urinary tracts by India ink injection revealed no sign of physical obstruction: ink flowed down the ureter into the bladder (Fig. 7I,J), although some regions with a very narrow lumen were observed. Similarly, *Six1*$^{-/-}$ ureters also had a very thin lumen in some areas as revealed by histological analysis (data not shown). This indicates that hydroureter and hydronephrosis were caused by functional, not anatomical, obstruction, and most likely because of ureteral SM malfunction.

We further determined whether the hydroureter and hydronephrosis observed in *Eya1*$^{Six1/+}$;*Six1*$^{-/-}$ mice resulted from impaired ureter peristalsis by culturing E14.5 ureters in medium for 3-5 days. Peristaltic contractions were observed after 3 days in culture from the proximal end of the ureter and progressed down the length of the ureter to the bladder in control samples (see Movie 1 in the supplementary material). Consistent with previous observations (Bush et al., 2006), cultured *Six1*$^{-/-}$ (see Movie 2 in the supplementary material) or *Eya1*$^{Six1/+}$;*Six1*$^{-/-}$ (see Movie 3 in the supplementary material) ureters also had peristaltic contractions, but the contractile waves appeared much weaker and smaller as judged by bright-field microscopy or by tracing the epithelial *Hoxb7-GFP* (Srinivas et al., 1999) under the microscope. Thus, we obtained direct evidence that abnormal SM formation caused by a lack of *Six1*

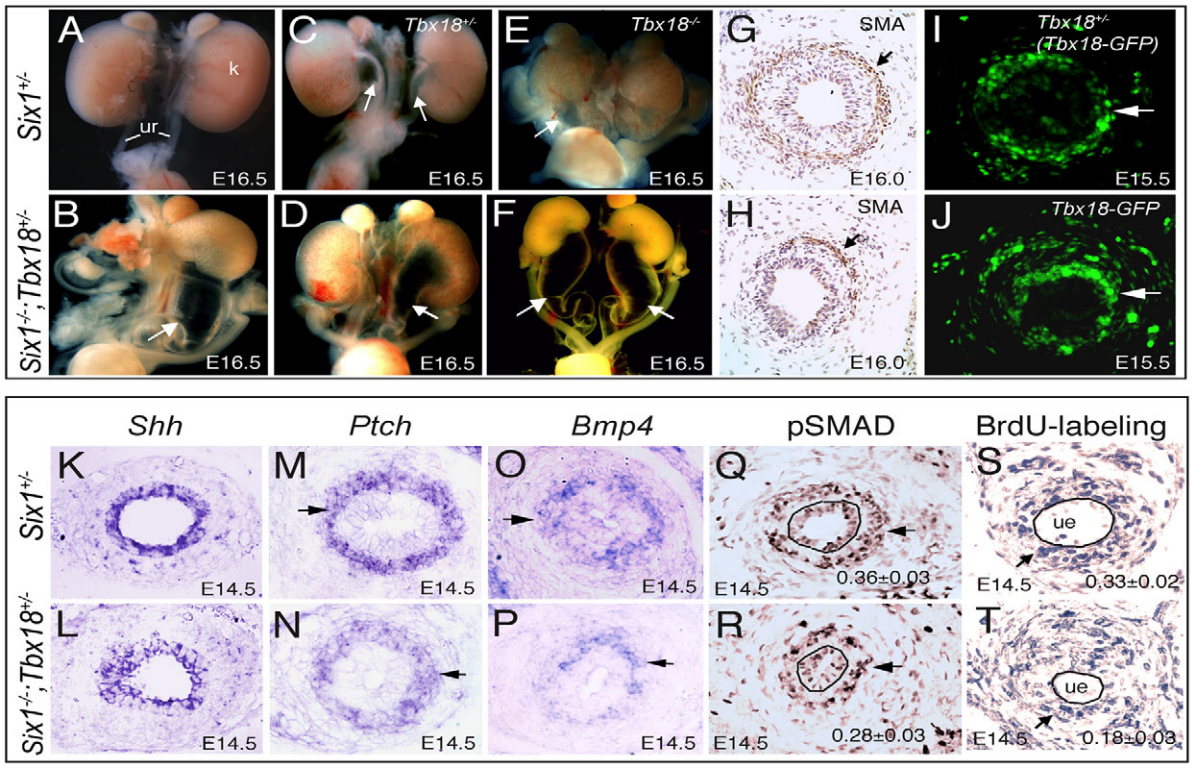

Fig. 8. *Six1* and *Tbx18* genetically interact during ureter development. (**A-F**) Urogenital systems in (A) *Six1*$^{+/-}$, (B,D,F) *Six1*$^{-/-}$;*Tbx18*$^{+/-}$, (C) *Six1*$^{+/-}$;*Tbx18*$^{-/-}$ and (E) *Six1*$^{-/-}$;*Tbx18*$^{-/-}$ mouse embryos. Arrows point to dilated ureters. Note the severe dilation in *Six1*$^{-/-}$;*Tbx18*$^{+/-}$ embryos. (**G**,**H**) Immunostaining for SMA on *Six1*$^{+/-}$ (G) and *Six1*$^{-/-}$;*Tbx18*$^{+/-}$ (H) transverse sections. (**I**,**J**) Transverse sections of ureters of *Six1*$^{+/-}$;*Tbx18*$^{+/-}$ (*Tbx18*$^{+/GFP}$) and *Six1*$^{-/-}$;*Tbx18*$^{+/-}$ embryos showing *Tbx18-GFP* expression in the ureteral mesenchyme. Arrows indicate condensing progenitors. Note that more *Tbx18-GFP*-positive cells were distributed in the outer layer in the *Six1*$^{-/-}$;*Tbx18*$^{+/-}$ mutant than in the *Six1*$^{+/-}$;*Tbx18*$^{+/-}$ control ureters. (**K-P**) In situ hybridization for *Shh*, *Ptch1* and *Bmp4* on transverse sections. (**Q**,**R**) Immunohistochemistry for pSMAD on transverse sections from *Six1*$^{+/-}$ and *Six1*$^{-/-}$;*Tbx18*$^{+/-}$ embryos. Arrows point to pSMAD-positive nuclei in the condensing mesenchyme. pSMAD-positive cells from five sections from each ureter (three ureters) were quantified as the ratio of pSMAD-positive cells to the total number of condensing mesenchymal cells in the control and mutant ureters. *P*-values (*P*=0.1039) were calculated using StatView *t*-test. (**S**,**T**) Transverse sections showing BrdU-positive cells (arrows). Proliferative rate was quantified as the ratio of BrdU-labeled cells to the total number of cells in the condensing mesenchyme from six sections from each ureter (from at least four ureters) on a radial plane. *P*-values (*P*=0.003) were calculated using StatView *t*-test. ue, urothelium.

in the ureter impairs ureteric peristalsis, providing a possible explanation for the hydroureter and hydronephrosis phenotype. In summary, these results provide definitive evidence that *Six1* plays an essential role in ureteral SM formation and function.

Six1 interacts with *Tbx18* to synergistically regulate ureter development

Since *Six1* expression overlaps with that of *Tbx18* in undifferentiated mesenchymal precursors from early stages (Airik et al., 2006), we examined whether *Six1* interacts with *Tbx18* to regulate ureter morphogenesis by generating *Six1;Tbx18* compound mutant mice. *Six1*$^{+/-}$;*Tbx18*$^{+/-}$ (*Tbx18*$^{+/GFP}$) double-heterozygous mice were of normal appearance and fertile. However, when examined at E16.5, around one-third of these mice displayed mild proximal hydroureter (8/27) (Fig. 8B), which was not observed in the single-heterozygote littermate controls (Fig. 8A). Strikingly, ~54% of *Six1*$^{-/-}$;*Tbx18*$^{+/-}$ mice (13/24) showed unilateral or bilateral hypoplastic kidneys (Fig. 8E-G), in contrast to only unilateral rudimentary kidneys in ~24% of *Six1*$^{-/-}$ mice (7/29). When the kidney was present in *Six1*$^{-/-}$;*Tbx18*$^{+/-}$ mice, hydroureter was frequently observed (~81%, 21/26), but never in the *Six1*$^{-/-}$ single mutant. The hydroureter phenotype, in most cases, was seen throughout the ureter and appeared to be much more severe (Fig. 8E-G) than in the *Eya1*$^{Six1/+}$;*Six1*$^{-/-}$ mutant (Fig. 7B). Moreover, the penetrance of the hydroureter and hydronephrosis phenotype was significantly higher in *Six1*$^{-/-}$;*Tbx18*$^{+/-}$ than in *Eya1*$^{Six1/+}$;*Six1*$^{-/-}$ embryos (~81% versus ~56%). By contrast, *Six1*$^{+/-}$;*Tbx18*$^{-/-}$ embryos exhibited a similar shortened ureter phenotype to that observed in *Tbx18*$^{-/-}$ single-mutant embryos (Fig. 8C) (Airik et al., 2006). Double-homozygous embryos at E16.5 (*n*=4) displayed variable renal defects, including renal agenesis and bilateral hypoplastic kidneys; however, the ureter SM was never formed (data not shown). In summary, these results show that *Six1* genetically interacts with *Tbx18* during ureter development and one-copy reduction of the *Tbx18* gene enhances the ureter defects associated with *Six1* deficiency.

We next examined the expression of marker genes to determine whether *Six1* and *Tbx18* act synergistically to regulate ureteral SM development. *SM22α* and SMA staining revealed that SM differentiation was more severely affected in the compound mutant than in the *Six1*$^{-/-}$ or *Eya1*$^{Six1/+}$;*Six1*$^{-/-}$ ureter before and after the onset of hydroureter. Specifically, SM differentiation as judged by SMA staining was delayed, being undetectable before E16.0, and the SM layer was very thin and often discontinuous at E16.0, before the onset of hydroureter (Fig. 8H, compare with 8G), and at E16.5 (data not shown). As the *Tbx18* mutant allele contains the *eGFP* reporter, we examined *Tbx18* expression by detecting *GFP*-positive

cells. Section examination at E15.5 showed that in the mutant, more *GFP*-positive cells were distributed outside of the condensing SM layer (Fig. 8J) than in controls (Fig. 8I), suggesting a recruitment/condensation defect. Examination of *Shh* expression in the epithelium revealed that in the compound mutant, *Shh* expression in some regions was reduced, although some epithelial cells still expressed *Shh* at levels similar to those in controls (Fig. 8K,L). The expression levels of *Ptch1* and *Bmp4* in the mesenchyme at E14.5 were decreased in the compound mutant (Fig. 8M-P). Further examination of pSMAD expression showed that pSMAD-positive cells were reduced in number in the condensing SM layer in the compound mutant (Fig. 8R) compared with controls (Fig. 8Q). These results suggest that *Six1* might act cooperatively with *Tbx18* to regulate the SHH and BMP signaling pathways during condensation/aggregation of the ureteral mesenchymal progenitors.

Since reduced proliferation of ureteral mesenchymal progenitors has been observed in *Tbx18*$^{-/-}$ embryos (Airik et al., 2006), we performed BrdU-incorporation experiments to further examine whether *Six1* acts together with *Tbx18* to regulate cell proliferation in the ureteral mesenchyme. Our results show that proliferation of ureteral SM progenitors was greatly reduced in *Six1*$^{-/-}$;*Tbx18*$^{+/-}$ ureters at E14.5 (Fig. 8R, arrow; 0.18±0.03 BrdU^{+} cells/total number of cells) when compared with controls (Fig. 8Q; 0.33±0.02 BrdU^{+} cells/total number of cells). Thus, *Six1* appears to genetically interact with *Tbx18* to regulate proliferation of ureteral SM progenitors.

SIX1 and TBX18 form a complex in cultured cells and developing ureters

Since *Six1* is co-expressed with *Tbx18* and these two genes genetically interact during ureter development, we tested whether their gene products physically interact by performing a co-IP analysis. Cell extracts from HEK 293 cells transfected with mouse *Six1* and *Flag-Tbx18* (FLAG tag added to the N-terminus of TBX18) or *Tbx18-Flag* (FLAG tag added to the C-terminus of TBX18) were incubated with FLAG antibody-coupled agarose beads and analyzed by western blotting with anti-SIX1 antibody. As shown in Fig. 9A, SIX1 co-immunoprecipitated with TBX18. We then examined whether the point mutations that cause single amino acid substitutions in the human *SIX1* gene from BOR patients (Ruf et al., 2004) affect SIX1-TBX18 complex formation. Interestingly, the single amino acid substitution of R110W located in the conserved SIX-specific domain decreased SIX1-TBX18 complex formation (Fig. 9B), whereas the single amino acid substitution of Y129C located in the conserved homeodomain completely abolished SIX1-TBX18 interaction. Although the Y129C mutation yielded a slightly smaller product in HEK 293 cells, because this mutant protein can be recognized by the anti-SIX1 antibody (which was raised against the entire homeodomain region) and can also bind to the SIX1 DNA-binding elements at reduced levels (Ruf et al., 2004), we concluded that the Y129C substitution specifically affects the SIX1-TBX18 interaction. These results demonstrate that SIX1 physically interacts with TBX18 and that two missense mutations identified in human BOR patients affect SIX1-TBX18 complex formation.

To further confirm that these two proteins physically interact to form a complex in the developing ureter, we prepared cell extracts from E14.5 mouse ureters and performed a co-IP experiment. Indeed, SIX1 and TBX18 were co-immunoprecipitated with either an anti-SIX1 or anti-TBX18 antibody (Fig. 9C and data not shown). Together, these results demonstrate that SIX1 physically forms a complex with TBX18 in the developing ureter, thus providing new insights into the molecular mechanisms of the urinary tract defects that occur in BOR patients.

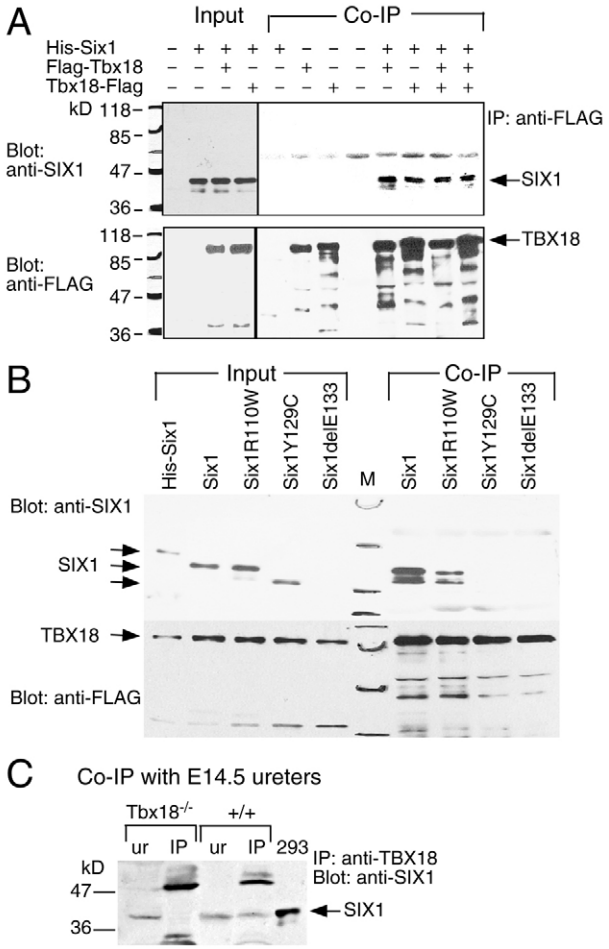

Fig. 9. SIX1 and TBX18 physically interact in vitro and in vivo. (**A**) Western blot and co-IP. Cell extracts (5 μg) from HEK 293 cells transfected with different combinations of *His-Six1/pcDNA3*, *Flag-Tbx18* or *Tbx18-Flag* were separated in SDS-PAGE gels and analyzed by western blotting with anti-SIX1 or anti-FLAG antibody to detect HIS-SIX1, FLAG-TBX18 or TBX18-FLAG. For co-IP experiments, ~0.4 mg of the same extracts was used. (**B**) Western blot and co-IP. Cell extracts (0.4 mg) from HEK 293 cells co-transfected with *His-Six1/pcDNA3*, *Six1/pcDNA*, its missense mutants (R110W, Y129C) or deletion mutant (delE133) and *Flag-Tbx18* were separated in SDS-PAGE gels and analyzed by western blotting with anti-SIX1 or anti-FLAG antibody to detect SIX1 or FLAG-TBX18.The antibody failed to detect the mutant delE133 protein. (**C**) Western blot and co-IP. Cell extracts (~3 mg) from E14.5 ureters were incubated with anti-TBX18 and precipitated by protein G-agarose beads. The precipitates were dissolved in SDS sample buffer followed by western blot analysis with anti-SIX1. ur, ureter; 293, cell lysates from HEK 293 cells transfected with *Flag-Tbx18* and *Six1*.

DISCUSSION

In this study, we examined the role of *Six1* during SM development in the ureter, which has not been previously explored. We have demonstrated that in the absence of *Six1*, ureter SMCs fail to form a cellular layer with normal SM architecture and function, this leading to hydroureter and hydronephrosis.

Six1 in ureter patterning and SM formation

Our results show that *Six1* is differentially expressed during ureter morphogenesis. In the developing ureter, *Six1* expression was observed in the undifferentiated mesenchymal cells that contribute

to the SM, the outer connective tissue and the stromal layers. Its expression was downregulated and eventually disappeared in the differentiating mesenchymal cells after E17.5 (Fig. 1). Analysis of *Six1*$^{-/-}$ ureters indicated that early events, such as condensation/aggregation and survival of the undifferentiated mesenchymal cells, were affected in the absence of *Six1*. In addition, the onset of SM differentiation was delayed in *Six1*$^{-/-}$ ureters. Subsequently, we observed abnormal expression of the SM-specific factors SMA, SM22α and SMMHC, indicating that ureteral SM differentiation is affected in *Six1*$^{-/-}$ embryos. These findings indicate that *Six1* has an early role in regulating SM formation.

So far, only two other transcription factors, TBX18 and TSHZ3, have been shown to be expressed in the undifferentiated ureteral mesenchyme. Loss-of-function studies in mice have indicated that *Tbx18* is required for progenitor cell development, whereas *Tshz3* is dispensable in the ureter before SM differentiation (Airik et al., 2006; Caubit et al., 2008). Deletion of *Tbx18* leads to failure of not only SM formation but also urothelium maturation, as well as to the absence of stromal marker expression (Airik et al., 2006). Inactivation of *Tshz3* results in a more specific defect of SMC differentiation without affecting the urothelium or the stromal cell layer (Caubit et al., 2008). How the ureteral SMC fate is determined remains poorly understood. In this study, we demonstrated that *Six1* and *Tbx18* act synergistically to regulate ureter morphogenesis.

During ureter development, *Tbx18* is specifically expressed in the ureteral mesenchyme from ~E11.5 and its expression remains high until E14.5, but is downregulated concomitantly with SM differentiation from E15.5 (Airik et al., 2006). This expression pattern overlaps with that of *Six1* (Fig. 1). However, as the onset of *Tbx18* expression appears to occur earlier than that of *Six1*, *Tbx18* might have a unique early role in the ureteral mesenchyme. This would explain why the ureter phenotype was much more severe in *Tbx18* than in *Six1* mutants. Nonetheless, the overlapping expression patterns of *Six1* and *Tbx18* in the ureteral mesenchyme suggests several possibilities as to their actions in regulating SM development. First, *Six1* might act synergistically with *Tbx18* in specifying or maintaining the ureteral mesenchymal progenitors. In the absence of the mesenchymal progenitors fated to become SMCs, no SM will form. This would explain why there was no SM formation in *Six1;Tbx18* double homozygotes (data not shown). Since our data show that the number of SM progenitors appeared to be increased on radial planes as labeled by *Tbx18* (Fig. 4), but that the number of differentiated SMCs was reduced in the *Six1*$^{-/-}$ ureter (Fig. 3), we speculate that some of these progenitors fail to acquire a SM fate. Upon failure to differentiate into SMCs, the progenitor cells undertake the cell death pathway, as detected by the TUNEL assay.

During ureteral SM formation, the mesenchymal progenitor cells proliferate longitudinally along with UB elongation. In *Six1*$^{-/-}$ ureters, more mesenchymal cells were observed on the radial axis and the shape of SMCs was irregular and disorganized. However, because the cell proliferation rate in the mutant was similar to that in control ureters, this might indicate that the expansion of mesenchymal cells on the radial plane is a secondary defect to the lack of a growing and ascending kidney in the *Six1*$^{-/-}$ mutant, which is the likely cause for the truncation of the ureters. Indeed, cell proliferation on the radial plane of *Eya1*$^{Six1/+}$*;Six1*$^{-/-}$ ureters that were of normal length appeared comparable to that in controls at E14.5-15.5 (data not shown). Although we failed to observe any obvious reduction in cell proliferation in the ureteral mesenchyme in *Six1*$^{-/-}$ or *Eya1*$^{Six1/+}$*;Six1*$^{-/-}$ ureters at E14.5-15.5, because reduced proliferation has been observed in several other organ systems of *Six1*$^{-/-}$ single-mutant embryos (Laclef et al., 2003; Xu et al., 2003; Zheng et al., 2003; Zou et al., 2006), it is possible that *Six1* cooperates with *Tbx18* to modulate cell proliferation during SM development. Indeed, proliferation of ureteral SM progenitors in *Six1*$^{-/-}$*;Tbx18*$^{+/-}$ embryos was reduced to ~54.5% of that of *Six1*-heterozygous controls at E14.5 (Fig. 8). Thus, *Six1* appears to act synergistically with *Tbx18* in regulating the proliferation of ureteral mesenchymal precursors.

During mesenchymal aggregation, a process that is disrupted in both *Tbx18*$^{-/-}$ (Airik et al., 2006) and *Six1*$^{-/-}$ (this study) mutants, the orientations and shapes of SMCs are rearranged resulting in spindle-shaped cells surrounding the epithelium, a process most likely regulated by subepithelial mesenchyme or *Bmp4*-expressing cells. In *Six1*$^{-/-}$ ureters, SHH and BMP4 signaling were normal, as assessed by the expression of *Shh*, *Ptch1*, *Bmp4* and pSMAD (Fig. 4 and data not shown). In addition, the expression of *Raldh2* in the stromal cells located between the SM and urothelium was also normal, suggesting that the abnormal SM formation observed in *Six1* mutants is a cell-autonomous defect. Thus, the mutant ureteral mesenchymal cells are probably incompetent to perceive signals from neighboring cells that are required for regulating SMC aggregation and maturation.

In contrast to *Six1*$^{-/-}$ ureters, loss of *Tbx18* in the ureteral mesenchyme not only affects the SMCs but also the stromal cells, as *Bmp4* and *Ptch1* expression was downregulated in the proximal region in the *Tbx18* mutant ureters at E12.5 (Airik et al., 2006). This is consistent with the idea that *Tbx18* has a unique early role in regulating ureter development. Our observation of a reduction in *Ptch1*, *Bmp4* and pSMAD expression in *Six1*$^{-/-}$*;Tbx18*$^{+/-}$ ureters suggests that *Six1* might cooperate with *Tbx18* in regulating epithelial-mesenchymal interactions during ureter patterning. Interestingly, loss of both genes in the mesenchyme also appears to affect urothelium differentiation (Figs 5, 6) (Airik et al., 2006). Unlike *Tbx18*, *Six1* expression was also observed in the urothelium from E18.5, which suggests that it might have a cell-autonomous role during urothelium maturation from around the newborn stage. However, because we observed abnormal cell death and disorganization of the urothelium from E15.5, which is almost 3 days before the onset of *Six1* expression in the urothelium, defects in the early events of ureteral mesenchyme development are most likely to affect urothelium development. We are currently using a conditional knockout approach to specifically delete *Six1* from the epithelial component or mesenchyme to investigate its roles in urothelium maturation and SM formation. Nonetheless, the *Six1* mutants provide a new mouse model for congenital ureter malformations and help us to understand the mechanisms that control ureter morphogenesis and SM formation. Because we found that these two proteins form a complex not only in cultured cells but also in developing ureters, *Six1* and *Tbx18* are likely to act together in the ureteral mesenchymal progenitors to regulate signaling pathways that control mesenchymal-epithelial interactions during ureter patterning.

It should be noted that *Six1* and *Tbx18* are unlikely to act in a linear cascade by regulating each other, as loss of either gene does not affect the expression of the other (Fig. 8J and data not shown). TBX18 and SIX1 are likely to act in parallel by forming a complex in the mesenchymal progenitors to regulate the expression of certain downstream genes. In future studies it will be important to identify their common downstream targets in the ureteral mesenchyme in order to understand their mode of action in controlling ureteral SM development.

SIX1 and hydroureter: new insight towards understanding the pathogenesis of the renal defects that occur in BOR syndrome

In this study, we demonstrated that a lack of *Six1* in the ureter leads to either bilateral or unilateral hydroureter from as early as E16.5 in the presence of a kidney restored by specifically expressing *Six1* in the MM (Fig. 7). Hydronephrosis was also observed, but this is likely to be a secondary defect of hydroureter as urinary flow blockage is thought to dilate the renal pelvis. Analysis of ureter morphology in $Six1^{-/-}$ or $Eya1^{Six1/+};Six1^{-/-}$ embryos at E18.5 revealed a continuous lumen along the entire ureter length and no physical obstruction was observed (Figs 2-7). Thus, it is very likely that the observed abnormal morphology and organization of SMCs is the major cause of hydroureter in the mutant. SMCs mediate the peristaltic movements that conduct the urine from the renal pelvis to the bladder, and $Six1^{-/-}$ ureters exhibited peristaltic movements (see Movies 1-3 in the supplementary material), consistent with previous observations (Bush et al., 2006). However, the peristaltic movements were much weaker in the $Six1^{-/-}$ ureters compared with controls. Such impaired peristalsis will lead to functional urine flow blockage. It is of interest to note that haploinsufficiency for human *SIX1* results in BOR syndrome, an autosomal dominant developmental disorder characterized by branchial clefts, hearing loss and renal anomalies (Abdelhak et al., 1997; Ruf et al., 2004). The renal defects observed in BOR patients include duplication or absence of the ureter, hydroureter or megaureter and hydronephrosis (Heimler and Lieber, 1986; Izzedine et al., 2004). Thus, the newly generated $Eya1^{Six1/+};Six1^{+/-}$ mice will serve as a new animal model for understanding the etiology of malformation of the ureter SM.

Previous studies have shown that loss of *Tbx18* leads to a severe form of hydroureter/hydronephrosis caused by a functional and partially physical ureter obstruction (Airik et al., 2006). Our results show that the two *SIX1* missense mutations identified from BOR patients that cause single amino acid substitutions reduced or abolished SIX1-TBX18 interactions. These results are also consistent with the observation that the two genes act synergistically during ureter morphogenesis, as severe hydroureter or megaureter was also observed in some $Tbx18^{+/-};Six1^{-/-}$ mice. Therefore, our results strongly suggest that the *SIX1* mutations in BOR patients are likely to influence the formation of the SIX1-TBX18 complex, thus causing the disease phenotype by affecting the expression of downstream genes.

Finally, an interesting finding of this work is that one-copy reduction of *Tbx18* substantially rescues $Six1^{-/-}$ kidney development. Previous work described that in addition to expression in the mesenchyme surrounding the ureteric stalk from ~E11.5, *Tbx18* is also expressed in the mesoderm next to the MM (Airik et al., 2006). We speculate that *Tbx18* modulates a signaling pathway that negatively regulates ureteric branching morphogenesis. As BMP4 signaling has a role in inhibiting ureteric branching but promoting ureter elongation, we hypothesize that loss of *Six1* in the MM leads to upregulation of BMP4 activity in the MM, which in turn inhibits UB branching but promotes its differentiation into ureter. Indeed, we found that one-copy reduction of *Bmp4* in $Six1^{-/-}$ embryos could restore kidney organogenesis but that hydroureter is also observed from as early as E16.5 (X.N., A. El-Hashash, J. Xu and P.-X.X., unpublished), similar to that observed in $Tbx18^{+/-};Six1^{-/-}$ mice. As *Bmp4* expression is eventually lost in *Tbx18*-null mice (Airik et al., 2006), it is possible that *Tbx18* is required for the maintenance of BMP4 activity in the mesenchyme, and one-copy reduction of *Tbx18* might cause a reduction in BMP4 activity in the mesenchyme that surrounds the proximal end of the UB, thus restoring kidney organogenesis by promoting branching morphogenesis in $Six1^{-/-};Tbx18^{+/-}$ embryos. In support of this view, BMP4 activity appears to be reduced in the ureteral mesenchyme in $Six1^{-/-};Tbx18^{+/-}$ embryos at E14.5 (Fig. 8).

In summary, in this work we provide definitive evidence that *Six1* has an essential role in ureter development. Our results strongly suggest that SIX1 acts as a co-transcription factor for TBX18 in ureteral mesenchyme development, thus providing new insights into the molecular basis of the urinary tract malformations in BOR patients.

Acknowledgements

We thank Dr Xiaogiang Cai for technical assistance on maintaining the *Tbx18* mutant mouse line, Dr Cathy Mendelsohn at Columbia University for kindly providing the *Radlh2* probe and Dr Tung-Tien Sun at New York University Medical School for the uroplakin antibody. This work was supported by NIH RO1 DK64640 (P.-X.X.). Deposited in PMC for release after 12 months.

Competing interests statement

The authors declare no competing financial interests.

Supplementary material

Supplementary material for this article is available at
http://dev.biologists.org/lookup/suppl/doi:10.1242/dev.045757/-/DC1

References

Abdelhak, S., Kalatzis, V., Heilig, R., Compain, S., Samson, D., Vincent, C., Weil, D., Cruaud, C., Sahly, I., Leibovici, M. et al. (1997). A human homologue of the Drosophila eyes absent gene underlies branchio-oto-renal (BOR) syndrome and identifies a novel gene family. *Nat. Genet.* **15**, 157-164.

Airik, R., Bussen, M., Singh, M. K., Petry, M. and Kispert, A. (2006). Tbx18 regulates the development of the ureteral mesenchyme. *J. Clin. Invest.* **116**, 663-674.

Brenner-Anantharam, A., Cebrian, C., Guillaume, R., Hurtado, R., Sun, T. T. and Herzlinger, D. (2007). Tailbud-derived mesenchyme promotes urinary tract segmentation via BMP4 signaling. *Development* **134**, 1967-1975.

Buller, C., Xu, X., Marquis, V., Schwanke, R. and Xu, P. X. (2001). Molecular effects of Eya1 domain mutations causing organ defects in BOR syndrome. *Hum. Mol. Genet.* **10**, 2775-2781.

Bush, K. T., Vaughn, D. A., Li, X., Rosenfeld, M. G., Rose, D. W., Mendoza, S. A. and Nigam, S. K. (2006). Development and differentiation of the ureteric bud into the ureter in the absence of a kidney collecting system. *Dev. Biol.* **298**, 571-584.

Cai, C. L., Martin, J. C., Sun, Y., Cui, L., Wang, L., Ouyang, K., Yang, L., Bu, L., Liang, X., Zhang, X. et al. (2008). A myocardial lineage derives from Tbx18 epicardial cells. *Nature* **454**, 104-108.

Cain, J. E., Hartwig, S., Bertram, J. F. and Rosenblum, N. D. (2008). Bone morphogenetic protein signaling in the developing kidney: present and future. *Differentiation* **76**, 831-842.

Carroll, T. J., Park, J. S., Hayashi, S., Majumdar, A. and McMahon, A. P. (2005). Wnt9b plays a central role in the regulation of mesenchymal to epithelial transitions underlying organogenesis of the mammalian urogenital system. *Dev. Cell* **9**, 283-292.

Caubit, X., Lye, C. M., Martin, E., Core, N., Long, D. A., Vola, C., Jenkins, D., Garratt, A. N., Skaer, H., Woolf, A. S. et al. (2008). Teashirt 3 is necessary for ureteral smooth muscle differentiation downstream of SHH and BMP4. *Development* **135**, 3301-3310.

Chen, B., Kim, E. H. and Xu, P. X. (2009). Initiation of olfactory placode development and neurogenesis is blocked in mice lacking both Six1 and Six4. *Dev. Biol.* **326**, 75-85.

Costantini, F. (2006). Renal branching morphogenesis: concepts, questions, and recent advances. *Differentiation* **74**, 402-421.

Dressler, G. R. (2006). The cellular basis of kidney development. *Annu. Rev. Cell Dev. Biol.* **22**, 509-529.

Heimler, A. and Lieber, E. (1986). Branchio-oto-renal syndrome: reduced penetrance and variable expressivity in four generations of a large kindred. *Am. J. Med. Genet.* **25**, 15-27.

Hosgor, M., Karaca, I., Ulukus, C., Ozer, E., Ozkara, E., Sam, B., Ucan, B., Kurtulus, S., Karkiner, A. and Temir, G. (2005). Structural changes of smooth muscle in congenital ureteropelvic junction obstruction. *J. Pediatr. Surg.* **40**, 1632-1636.

Hoskins, B. E., Cramer, C. H., Silvius, D., Zou, D., Raymond, R. M., Orten, D. J., Kimberling, W. J., Smith, R. J., Weil, D., Petit, C. et al. (2007). Transcription factor SIX5 is mutated in patients with branchio-oto-renal syndrome. *Am. J. Hum. Genet.* **80**, 800-804.

Izzedine, H., Tankere, F., Launay-Vacher, V. and Deray, G. (2004). Ear and kidney syndromes: molecular versus clinical approach. *Kidney Int.* **65**, 369-385.

Kuwayama, F., Miyazaki, Y. and Ichikawa, I. (2002). Embryogenesis of the congenital anomalies of the kidney and the urinary tract. *Nephrol. Dial. Transplant.* **17**, 45-47.
Laclef, C., Hamard, G., Demignon, J., Souil, E., Houbron, C. and Maire, P. (2003). Altered myogenesis in Six1-deficient mice. *Development* **130**, 2239-2252.
Li, X., Oghi, K. A., Zhang, J., Krones, A., Bush, K. T., Glass, C. K., Nigam, S. K., Aggarwal, A. K., Maas, R., Rose, D. W. et al. (2003). Eya protein phosphatase activity regulates Six1-Dach-Eya transcriptional effects in mammalian organogenesis. *Nature* **426**, 247-254.
Massague, J., Seoane, J. and Wotton, D. (2005). Smad transcription factors. *Genes Dev.* **19**, 2783-2810.
Michos, O., Goncalves, A., Lopez-Rios, J., Tiecke, E., Naillat, F., Beier, K., Galli, A., Vainio, S. and Zeller, R. (2007). Reduction of BMP4 activity by gremlin 1 enables ureteric bud outgrowth and GDNF/WNT11 feedback signalling during kidney branching morphogenesis. *Development* **134**, 2397-2405.
Miyazaki, Y., Oshima, K., Fogo, A., Hogan, B. L. and Ichikawa, I. (2000). Bone morphogenetic protein 4 regulates the budding site and elongation of the mouse ureter. *J. Clin. Invest.* **105**, 863-873.
Raatikainen-Ahokas, A., Hytonen, M., Tenhunen, A., Sainio, K. and Sariola, H. (2000). BMP-4 affects the differentiation of metanephric mesenchyme and reveals an early anterior-posterior axis of the embryonic kidney. *Dev. Dyn.* **217**, 146-158.
Ruf, R. G., Xu, P. X., Silvius, D., Otto, E. A., Beekmann, F., Muerb, U. T., Kumar, S., Neuhaus, T. J., Kemper, M. J., Raymond, R. M., Jr et al. (2004). SIX1 mutations cause branchio-oto-renal syndrome by disruption of EYA1-SIX1-DNA complexes. *Proc. Natl. Acad. Sci. USA* **101**, 8090-8095.
Sajithlal, G., Zou, D., Silvius, D. and Xu, P. X. (2005). Eya 1 acts as a critical regulator for specifying the metanephric mesenchyme. *Dev. Biol.* **284**, 323-336.
Saxen, L., Sariola, H. and Lehtonen, E. (1986). Sequential cell and tissue interactions governing organogenesis of the kidney. *Anat. Embryol. (Berl.)* **175**, 1-6.
Schedl, A. (2007). Renal abnormalities and their developmental origin. *Nat. Rev. Genet.* **8**, 791-802.
Shah, M. M., Sampogna, R. V., Sakurai, H., Bush, K. T. and Nigam, S. K. (2004). Branching morphogenesis and kidney disease. *Development* **131**, 1449-1462.
Srinivas, S., Goldberg, M. R., Watanabe, T., D'Agati, V., al-Awqati, Q. and Costantini, F. (1999). Expression of green fluorescent protein in the ureteric bud of transgenic mice: a new tool for the analysis of ureteric bud morphogenesis. *Dev. Genet.* **24**, 241-251.
Sun, T. T., Liang, F. X. and Wu, X. R. (1999). Uroplakins as markers of urothelial differentiation. *Adv. Exp. Med. Biol.* **462**, 7-18; discussion 103-114.
Wang, G. J., Brenner-Anantharam, A., Vaughan, E. D. and Herzlinger, D. (2009). Antagonism of BMP4 signaling disrupts smooth muscle investment of the ureter and ureteropelvic junction. *J. Urol.* **181**, 401-407.
Xu, P. X., Adams, J., Peters, H., Brown, M. C., Heaney, S. and Maas, R. (1999). Eya1-deficient mice lack ears and kidneys and show abnormal apoptosis of organ primordia. *Nat. Genet.* **23**, 113-117.
Xu, P. X., Zheng, W., Laclef, C., Maire, P., Maas, R. L., Peters, H. and Xu, X. (2002). Eya1 is required for the morphogenesis of mammalian thymus, parathyroid and thyroid. *Development* **129**, 3033-3044.
Xu, P. X., Zheng, W., Huang, L., Maire, P., Laclef, C. and Silvius, D. (2003). Six1 is required for the early organogenesis of mammalian kidney. *Development* **130**, 3085-3094.
Yu, J., Carroll, T. J. and McMahon, A. P. (2002). Sonic hedgehog regulates proliferation and differentiation of mesenchymal cells in the mouse metanephric kidney. *Development* **129**, 5301-5312.
Zheng, W., Huang, L., Wei, Z. B., Silvius, D., Tang, B. and Xu, P. X. (2003). The role of Six1 in mammalian auditory system development. *Development* **130**, 3989-4000.
Zou, D., Silvius, D., Davenport, J., Grifone, R., Maire, P. and Xu, P. X. (2006). Patterning of the third pharyngeal pouch into thymus/parathyroid by Six and Eya1. *Dev. Biol.* **293**, 499-512.